

NASA/TM-2014-218272



Mitigation of Crack Damage in Metallic Materials

Patrick E. Leser

North Carolina State University, Raleigh, North Carolina

John A. Newman, Stephen W. Smith, William P. Leser, Russell A. Wincheski,

Terryl A. Wallace, Edward H. Glaessgen, and Robert S. Piascik

Langley Research Center, Hampton, Virginia

May 2014

NASA STI Program . . . in Profile

Since its founding, NASA has been dedicated to the advancement of aeronautics and space science. The NASA scientific and technical information (STI) program plays a key part in helping NASA maintain this important role.

The NASA STI program operates under the auspices of the Agency Chief Information Officer. It collects, organizes, provides for archiving, and disseminates NASA's STI. The NASA STI program provides access to the NASA Aeronautics and Space Database and its public interface, the NASA Technical Report Server, thus providing one of the largest collections of aeronautical and space science STI in the world. Results are published in both non-NASA channels and by NASA in the NASA STI Report Series, which includes the following report types:

- **TECHNICAL PUBLICATION.** Reports of completed research or a major significant phase of research that present the results of NASA Programs and include extensive data or theoretical analysis. Includes compilations of significant scientific and technical data and information deemed to be of continuing reference value. NASA counterpart of peer-reviewed formal professional papers, but having less stringent limitations on manuscript length and extent of graphic presentations.
- **TECHNICAL MEMORANDUM.** Scientific and technical findings that are preliminary or of specialized interest, e.g., quick release reports, working papers, and bibliographies that contain minimal annotation. Does not contain extensive analysis.
- **CONTRACTOR REPORT.** Scientific and technical findings by NASA-sponsored contractors and grantees.

- **CONFERENCE PUBLICATION.** Collected papers from scientific and technical conferences, symposia, seminars, or other meetings sponsored or co-sponsored by NASA.
- **SPECIAL PUBLICATION.** Scientific, technical, or historical information from NASA programs, projects, and missions, often concerned with subjects having substantial public interest.
- **TECHNICAL TRANSLATION.** English-language translations of foreign scientific and technical material pertinent to NASA's mission.

Specialized services also include organizing and publishing research results, distributing specialized research announcements and feeds, providing information desk and personal search support, and enabling data exchange services.

For more information about the NASA STI program, see the following:

- Access the NASA STI program home page at <http://www.sti.nasa.gov>
- E-mail your question to help@sti.nasa.gov
- Fax your question to the NASA STI Information Desk at 443-757-5803
- Phone the NASA STI Information Desk at 443-757-5802
- Write to:
STI Information Desk
NASA Center for AeroSpace Information
7115 Standard Drive
Hanover, MD 21076-1320

NASA/TM-2014-218272



Mitigation of Crack Damage in Metallic Materials

Patrick E. Leser
North Carolina State University, Raleigh, North Carolina

*John A. Newman, Stephen W. Smith, William P. Leser, Russell A. Wincheski,
Terryl A. Wallace, Edward H. Glaessgen, and Robert S. Piascik*
Langley Research Center, Hampton, Virginia

National Aeronautics and
Space Administration

Langley Research Center
Hampton, Virginia 23681-2199

May 2014

Acknowledgments

The research described in this document was funded by the NASA Vehicle Systems Safety Technologies (VSST) Program. The authors wish to express gratitude to Rick Ross (VSST, Langley Research Center) for his efforts in supporting this research. One author (Patrick Leser) supported this research while participating in the Langley Aerospace Research Summer Scholar (LARSS) program as a graduate student at North Carolina State University. Another author (W.P. "Paul" Leser) supported this research while participating in the NASA Pathways program. Finally, the authors wish to express gratitude to the laboratory support provided by William T. "Tommy" Howard (NASA retired), Jim Baughman (Analytical Mechanics Association), H.D. "Clay" Claytor (Analytical Mechanics Association), Joel Alexa (Analytical Mechanics Association), and Greg Shanks (NASA). The work described in this document is covered by a U.S. patent (publication number: US8347479 B2, Title "Method for Repairing Cracks in Structures," publication date: January 8, 2013).

Available from:

NASA Center for AeroSpace Information
7115 Standard Drive
Hanover, MD 21076-1320
443-757-5802

Abstract

A system designed to mitigate or heal crack damage in metallic materials has been developed where the protected material or component is coated with a low-melting temperature film. After a crack is formed, the material is heated, melting the film which then infiltrates the crack opening through capillary action. Upon solidification, the healing material inhibits further crack damage in two ways. While the crack healing material is intact, it acts like an adhesive that bonds or bridges the crack faces together. After fatigue loading damages, the healing material in the crack mouth inhibits further crack growth by creating artificially-high crack closure levels. Mechanical test data show that this method successfully arrests or retards crack growth in laboratory specimens.

Introduction

Damage tolerance concepts have been applied to aerospace vehicles for decades to improve safety. Here, the remaining service life is calculated using fatigue crack growth models based on service loads, material, component geometry, and crack size as determined from periodic vehicle inspections. If no cracks are detected, the largest crack that could escape detection, based on the probability of detection (POD) for the inspection method used, is assumed to exist. The remaining useful service life can then be calculated and used to establish inspection intervals such that multiple inspections would be performed as a crack propagates from an inspection threshold to a critical size (*i.e.*, where component failure would occur). This damage tolerance methodology has proven very successful for many applications but is not yet practical for all aerospace components, especially components that are difficult to inspect and those subjected to high-cycle fatigue loading. For high-cycle fatigue loading, the number and severity of load cycles per flight hour is such that the portion of service life with a detectable crack is too small to be divided into practical inspection intervals. A novel solution to this issue is provided by the authors, where fatigue cracks are “healed” by the introduction of a foreign material into the crack mouth, thus slowing or even stopping crack growth and extending the portion of service life associated with the propagation of microstructurally-long cracks (ref. 1). When a crack is detected on an aerospace structure via a diagnostic sensor network or through nondestructive evaluation (NDE), the healing material, which has been applied directly to the structural material as a thin-film coating, is locally activated by heat, allowing the healing material to flow into the crack, as depicted in Figure 1a. Upon solidification, the coating reduces the crack driving force by adhering the crack surfaces together, a mechanism termed “crack bridging” (see Figure 1b) and by leaving voluminous material in the crack wake, an artificial form of crack closure (see Figure 1c).

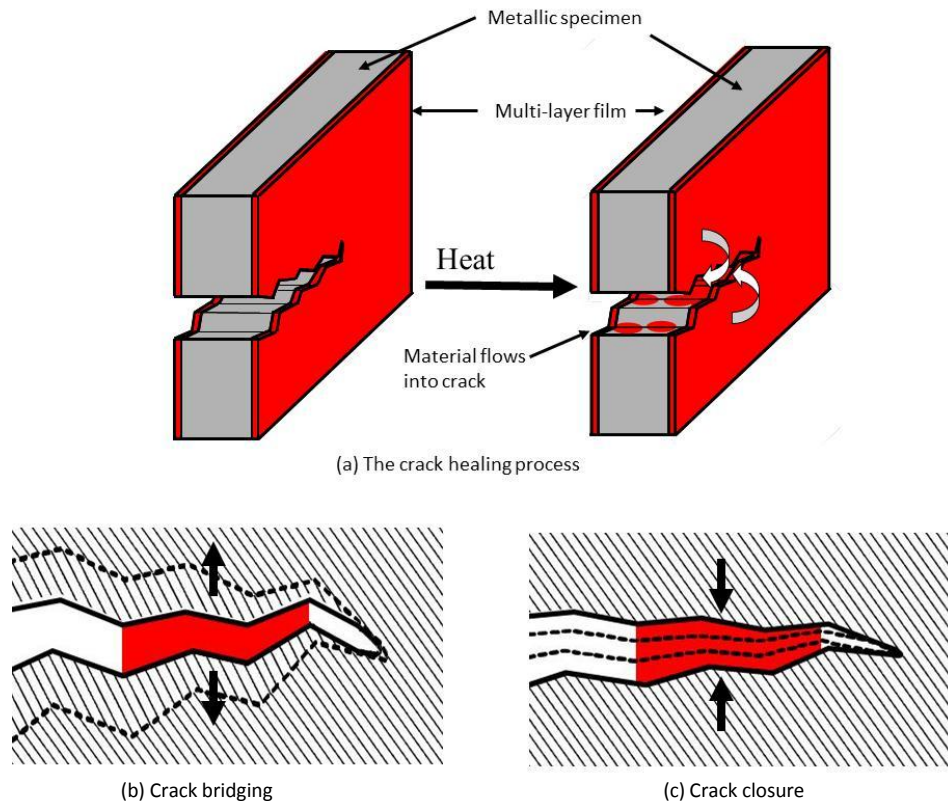


Figure 1. A schematic of the crack healing procedure is shown. The dotted lines represent the profile of the crack without the presence of healing material in the mouth.

Previous crack healing efforts

The alleviation of crack damage in structures is mostly limited to invasive and costly maintenance methods (e.g., patching). If the damage is too severe or too many repairs have been made previously, total component replacement is required. These types of repairs contribute to aircraft empty weight since excess material is almost always required to perform a safe repair (ref. 2). It is for these reasons that investigations into new, low-weight methods to treat or “heal” damage with minimal invasiveness have begun to emerge. Many advances have already been made in self-healing composites and polymers (refs. 3-8), but the primary methods used in these fields to deliver the healing agent to the damaged area are not applicable to metals or alloys due to the difficulties and impracticalities of embedding in a metallic matrix (ref. 9). As a result, it was not until recently that researchers began to focus on the self-healing of metallic materials. Manuel, *et al.*, developed a method that involved the introduction of shape memory alloy (SMA) wires into a metallic matrix (refs. 10-12). Upon crack propagation, the SMA wires were used to induce crack closure, pulling the crack surfaces together and applying a compressive force. The entire specimen was then heated until limited surface melting occurred; after cooling, the matrix crack had been essentially removed. While the method seems promising, it is currently not applicable to “commonly used” metals and

alloys, such as aerospace-grade aluminum and titanium (refs. 10-12). Another proposed healing method includes the delivery of a healing agent via embedded ceramic tubes that are exposed by crack propagation and activated through heating (ref. 13). As mentioned previously, the complexity of an embedded network to deliver the healing agent presents complications, primarily through degradation to the overall metallic material properties as well as manufacturing challenges.

Solid state self-healing concepts have also been proposed. One such method involves the self-healing of underaged aluminum through dynamic precipitation (*i.e.*, solute transported to open volumes, such as internal cracks and voids) during creep and fatigue (refs. 14-16). Further contributions were made with positron annihilation spectroscopy studies, which allowed for a deeper understanding of how solute atoms are driven to areas where crack initiation may occur (refs. 17, 18). However, a study by Wanhill (ref. 19) suggests that precipitate-based solid state healing is not practical for real-world aerospace applications. He argues that most aircraft damage will either be too large to be healed by dynamic precipitation (which is mostly limited to healing slip band cracks on the scale of 1.4 μm or smaller) or will be located on the surface of the component, where environmental effects could potentially hinder crack healing (ref. 19).

Proposed healing agent

The proposed crack healing process described previously (Figure 1) is novel in that it is designed for metallic materials and, because it relies on a surface coating, is readily applicable to existing aerospace components. Since this method is intended for aerospace metallic materials (*e.g.*, aluminum and titanium), the healing material is to have a melting temperature well below that which would cause aging of the protected structural material over any potential healing times. For this study, the selected healing film was a near-eutectic composition of Indium-Tin (In-Sn), which was roughly 60% Indium and 40% Tin by weight (ref. 20). As seen in the phase diagram of the In-Sn system, given in Figure 2, the melting temperature of the target healing material is approximately 124°C. Since the sputtering process is based on momentum transfer and In and Sn vary in atomic weight by 2%, a slight variation in initial and deposited chemistry is expected. The 60/40 In-Sn chemistry, which is slightly Indium rich of the eutectic composition, was selected to reduce the possibility of creating a local Tin-rich chemistry, which would increase the melting point significantly as a function of composition. In contrast, the Indium-rich side of the eutectic composition has a shallow liquid-solid slope and is generally more forgiving.

Specimen Preparation

Fatigue crack growth testing was done using the eccentrically-loaded single-edge notch tension (ESE(T)) specimen (refs. 21, 22). A schematic of the ESE(T) specimen is shown in Figure 3. Testing described in this document was done with specimens made from Titanium alloy 6-2-2-2 sheet material approximately 0.080 inches (2.03 mm) thick. After machining by EDM wire, specimen surfaces were mechanically polished to a near-mirror finish on both sides before a back-face strain gage was applied to the specimen. Back-face strain gages were used to monitor crack length during fatigue crack growth testing (refs. 23, 24). The In-Sn healing material was then deposited on either one or two sides of the specimen using a radio frequency

(RF) sputter deposition technique. A deposition rate of $\sim 1 \mu\text{m/hr}$ for 5-15 hours was used with a power of 250 W in 1.1 Pa (8 mTorr) Argon environment, resulting in film thicknesses on the order of $\sim 5\text{-}15 \mu\text{m}$. Upon completion of the film deposition, the specimens were annealed at 135°C for thirty minutes to help consolidate the film. A more detailed description of the sputter coating process and characterization efforts of the resulting healing film is given in the Appendix.

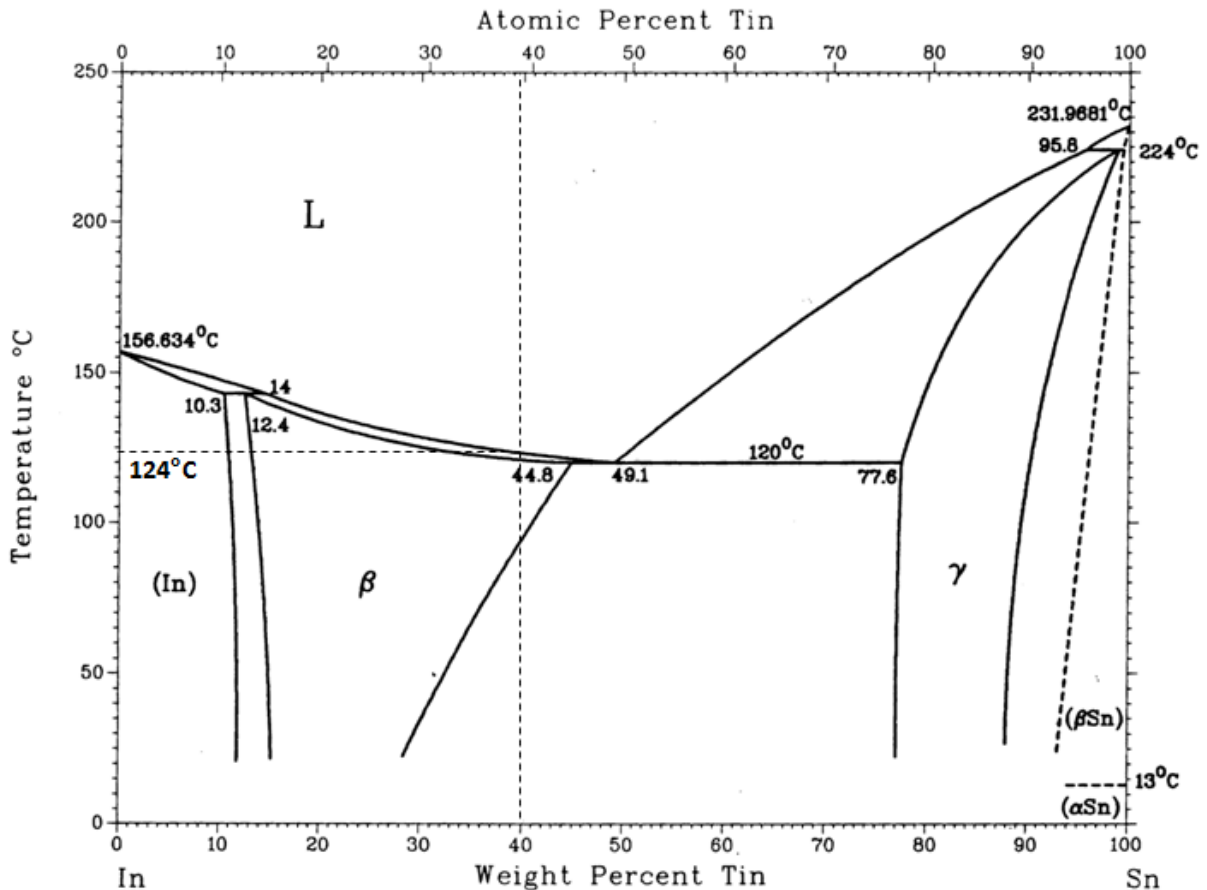


Figure 2. Phase diagram for Indium-Tin system (ref. 2). The target composition (60/40 In-Sn) used in this study is indicated by a dashed line.

Fatigue Crack Growth Test Procedure

Fatigue crack growth testing was done in accordance with ASTM Standard E647 (ref. 22), with a computer-controlled servo-hydraulic test machine, where a back-face strain gage was used to determine crack length. Applied loads were continuously adjusted, based on crack length, such that programmed stress intensity factors were achieved. To best characterize the effects of crack healing, constant- ΔK testing was performed; here, the crack-tip driving force

parameter, ΔK , was held constant as the crack propagated across the specimen. Fatigue loading was performed in this study at a load ratio (ratio of minimum to maximum applied loads) of $R = 0.1$. For homogenous materials, this test method is expected to produce constant crack growth rates such that a plot of crack length versus applied load cycle count should be a straight line (refs. 25, 26). Even subtle variations in crack growth rate can be determined using constant- ΔK testing. Due to oxidation concerns of the In-Sn healing material, testing was performed in an evacuated vacuum chamber ($<1.3 \cdot 10^{-6}$ Pa, $<10^{-8}$ Torr). After crack healing, the In-Sn material in the crack mouth affects the compliance-based crack length such that the automated test system perceives a reduction in crack length to have occurred. Should a constant- ΔK be programmed at this time, a significant increase in load would occur (due to the shorter compliance-based crack length). Since the actual crack length has not decreased, this is not desirable; therefore, fatigue loading is resumed at the loads corresponding to that just before crack healing was initiated. Constant- ΔK testing was resumed after the compliance-based crack length grew to the pre-healed value. A photograph of the test setup is shown in Figure 4.

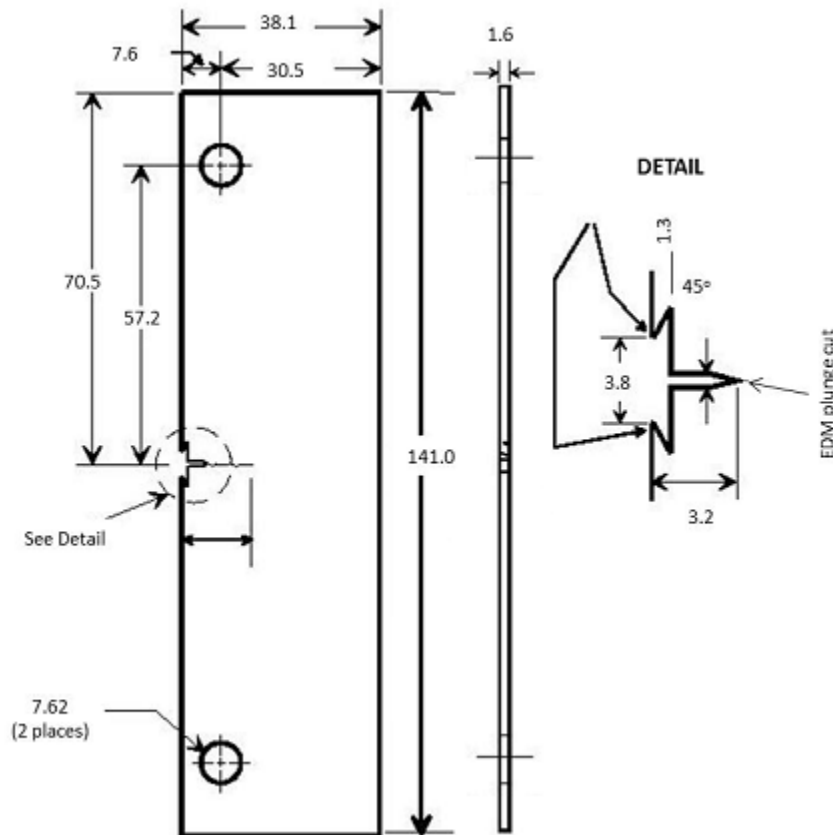


Figure 3. Schematic of the ecentrically-loaded single-edge notch tension (ESE(T)) specimen configuration. All dimensions in millimeters (mm).

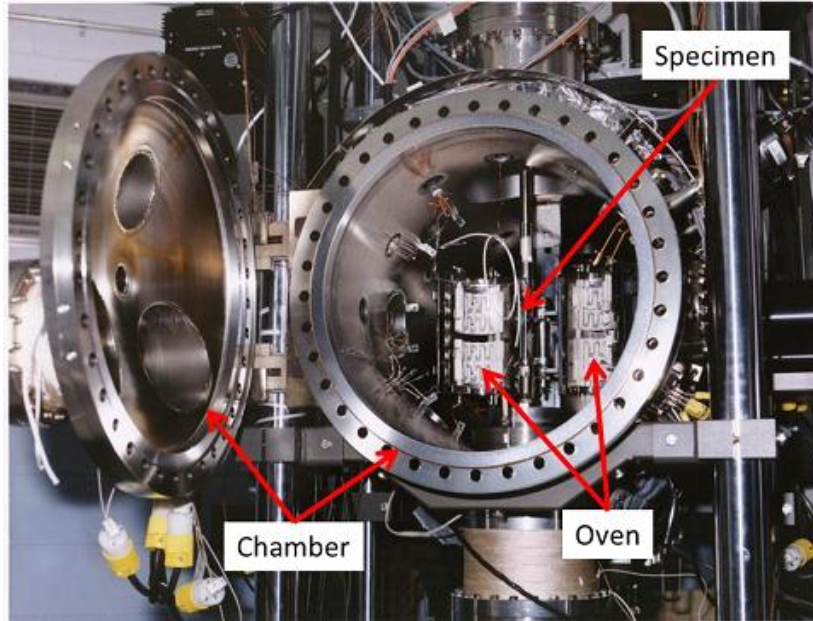


Figure 4. Photograph of the test setup.

Crack healing tests were run in multiple steps. First, a steady-state fatigue crack growth rate was achieved over a crack growth increment of at least 1.3 mm (0.050 inches). Then, the fatigue loading was stopped while the specimen was held at a constant load of approximately 90% of the maximum cyclic load and heated to 135°C (275°F) for approximately 1 hour. It is not believed that transport of the healing material into the crack mouth requires a great deal of time, but an hour was allowed to ensure that the entire specimen reached a thermal steady state greater than the melting temperature of the healing film. This process will be investigated further in future studies. Small, molten metallic spheres observed on the specimen surface during heating were believed to be evidence that melting of the film (or at least a significant portion of it) had occurred. A photograph of these metallic spheres is shown in Figure 5. After heating for 1 hour, the specimen was allowed to cool to ambient temperature, and then fatigue loading was resumed.

Fatigue Crack Growth Results

The results of two fatigue crack growth tests performed at constant- ΔK values of (a) 6.6 MPa $\sqrt{\text{m}}$ and (b) 13.2 MPa $\sqrt{\text{m}}$ are shown in Figure 6. When constant- ΔK test data are plotted as crack-length-versus-cycle-count, the slope of the data is the fatigue crack growth rate. Consider the test run at the lower ΔK value ($\Delta K = 6.6 \text{ MPa}\sqrt{\text{m}}$); the steady state fatigue crack growth rate data (for the inert environment) are shown as solid circular symbols. These data form a nearly-straight line indicating that steady-state crack growth occurred between crack lengths of $a = 6.9 \text{ mm}$ (0.27 inches) and $a = 9.9 \text{ mm}$ (0.39 inches). The crack growth rate of $da/dN = 1.96 \times 10^{-9} \text{ m/cycle}$ ($7.7 \times 10^{-8} \text{ inch/cycle}$) is indicated in the figure. At a crack length of $a = 9.9 \text{ mm}$ (0.39 inches), cyclic loading was paused while the healing film was activated (heated and cooled as previously described). After the specimen cooled to ambient temperature and solidification of the healing material occurred, cyclic loading was resumed at constant load. The crack length,

based on compliance data, appeared to have decreased to a value of approximately $a = 9.9$ mm (0.30 inches).¹ After approximately 1 million load cycles, the compliance-based crack length increased slightly to approximately $a = 8.4$ mm (0.33 inches) (open circular symbols). Presumably, this increase in compliance-based crack length is a result of damage to the healing material in the crack mouth. Further cyclic loading resulted in negligible crack growth; the near-horizontal line between 3 million and 4.5 million load cycles indicates that the crack growth rate was nearly zero ($da/dN = 0$). This suggests that no further damage to the healing material occurred and crack arrest was achieved. If the healing material was not introduced to the crack, the crack would have continued to propagate at a constant rate as indicated by the dashed line in Figure 6a.

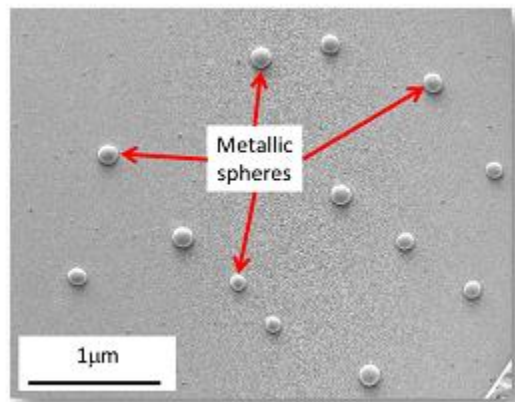


Figure 5. Photograph of the In-Sn healing film after thermal cycling. The metallic spheres, which suggest that initial melting of the film has occurred, are indicated.

Next, consider the test run at the higher ΔK value ($\Delta K = 13.2$ MPa $\sqrt{\text{m}}$, twice the crack-tip loading of Figure 6a). The steady state fatigue crack growth rate data (for the inert environment) are shown as solid circular symbols. These data form a nearly-straight line indicating that steady-state crack growth occurred between crack lengths of $a = 12.2$ mm (0.48 inches) and $a = 14.5$ mm (0.57 inches). The crack growth rate of $da/dN = 5.08 \times 10^{-8}$ m/cycle (2.0×10^{-6} inch/cycle) is indicated in the figure. At a crack length of $a = 14.5$ mm (0.57 inches), cyclic loading was paused while the healing film was activated (heated and cooled as previously described). After the specimen cooled to ambient temperature, and solidification of the healing

¹ Recall that crack length is determined from compliance data measured from a strain gage on the specimen back face. The reduction in crack length is due to the presence of the healing material in the crack mouth affecting the specimen compliance. It is believed that the crack length nearly returning to the original value where the crack started suggests that the healing material has adhered to nearly the entire crack surface that was produced in the inert environment. Considering that the crack is not truly "healed," and that the crack-tip loading is a function of applied load and crack length, the applied load corresponding to the crack length at the initiation of the healing process (here, $a = 9.91$ mm (0.39 inches)) was maintained.

material occurred, cyclic loading was resumed. Without healing, the crack would have continued to propagate as indicated by the red dashed line in the figure; instead, the crack length, based on compliance data, appeared to have decreased to a value of approximately $a = 8.1$ mm (0.32 inches). It should be noted here that the tests associated with Figures 6a and 6b were run on the same specimen.² After approximately 8,000 load cycles, the compliance-based crack length returned to the crack length before the healing material was heated ($a = 14.5$ mm (0.57 inches)). Presumably, this rapid increase in compliance-based crack length (open circular symbols) is a result of damage to the healing material in the crack mouth, destroying the crack bridging capability of the healing material. Further cyclic loading resulted in negligible crack growth for approximately 200,000 additional load cycles, as indicated by the near-horizontal line between 100,000 and 300,000 load cycles (*i.e.*, temporary crack arrest was attained). After 300,000 load cycles, the crack began to propagate, but did so at about 45% of the original crack growth rate ($da/dN = 2.26 \times 10^{-8}$ m/cycle (8.9×10^{-7} inches/cycle)). High crack closure loads measured during the test strongly suggest that the decrease in crack growth rates were a result of the artificially-high crack closure effect of the residual healing material in the crack wake. Compliance-based data suggested that the crack closure levels were initially high, with crack closure loads greater than 50% of the maximum load, and tended to decrease as the crack propagated. Typical crack closure loads before healing were nearly 25% of the maximum load.

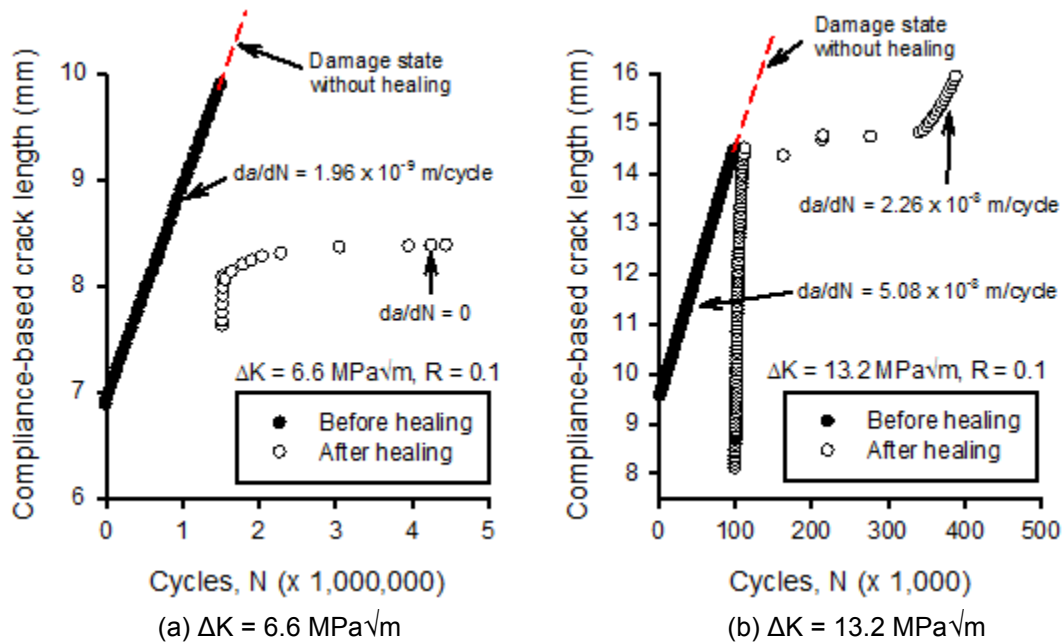


Figure 6. Plots of fatigue crack growth data for titanium specimens during healing tests.

² After precracking in air, both tests were run in vacuum without exposing the fresh crack surfaces to an oxygen-rich environment. Here, the crack appears to have healed to a compliance-based crack length corresponding to the end of specimen precracking in air, covering the crack surfaces of both tests generated in an inert environment.

Discussion of Results

The results shown in Figure 6 indicate that the crack healing method developed by the authors is capable of arresting fatigue crack growth at low ΔK (*i.e.*, $\Delta K = 6.6 \text{ MPa}\sqrt{\text{m}}$). Although the results show that crack arrest is temporary at higher ΔK values (*i.e.*, $\Delta K = 13.2 \text{ MPa}\sqrt{\text{m}}$), there was still a significant benefit from the crack healing process. Presumably, at low ΔK the healing material remained intact, preserving the crack bridging capability of the crack-mouth healing material. At higher ΔK values, the crack-mouth healing material was ruptured such that crack growth eventually resumed; however, the subsequent crack growth occurred at a much lower crack growth rate. The reduction in crack growth rate coinciding with high crack closure levels strongly suggests that the residual healing material in the crack wake created artificially high crack closure levels. Considering that the fracture toughness of aerospace titanium alloys is nearly $50 \text{ MPa}\sqrt{\text{m}}$, the inability to arrest cracks above $13 \text{ MPa}\sqrt{\text{m}}$ might suggest that this crack healing method is of limited use; however, the nature of crack growth is that cracks typically spend the majority of their lives slowly propagating small cracks at low ΔK conditions (*i.e.*, near-threshold fatigue crack growth). Furthermore, since a single specimen was healed twice, as demonstrated in Figure 6, repeatability has been demonstrated in that a healing film is reusable even after the first healing attempt.

The evidence is clear that the crack healing material flows into the crack mouth based on X-ray Computed Tomography (CT) and Energy Dispersive Spectroscopy (EDS) scans, which are presented in Figure 7a and 7b, respectively, for a typical healed crack growth specimen. An X-ray CT scan of a healed specimen is shown in Figure 7a; here, the In-Sn healing material can be seen as the light colored region where the specimen is viewed normal to the plane of the crack. In this case, the healing material appears to coat nearly the entire crack surface, from one surface to the other and all the way to the crack tip. After healing, some specimens were loaded to failure, exposing the crack surfaces for study. EDS scans were conducted on the exposed crack surfaces producing the color-coded maps shown in Figure 7b. Coverage of Indium (In) and Tin (Sn) on the crack growth surface produced during the test (in an inert environment) and the absence of these elements on the crack surfaces produced as the specimen was overloaded also suggests that the material infiltrated the crack mouth successfully during the healing process. However, careful examination of the In and Sn coverage reveals that the crack surface was less-than-uniformly coated with the In-Sn healing material, perhaps because this material seems to have infiltrated the crack opening only at a few discrete locations; these locations can be identified as points where the healing material on the surface of the specimen meets the material on the crack surface.

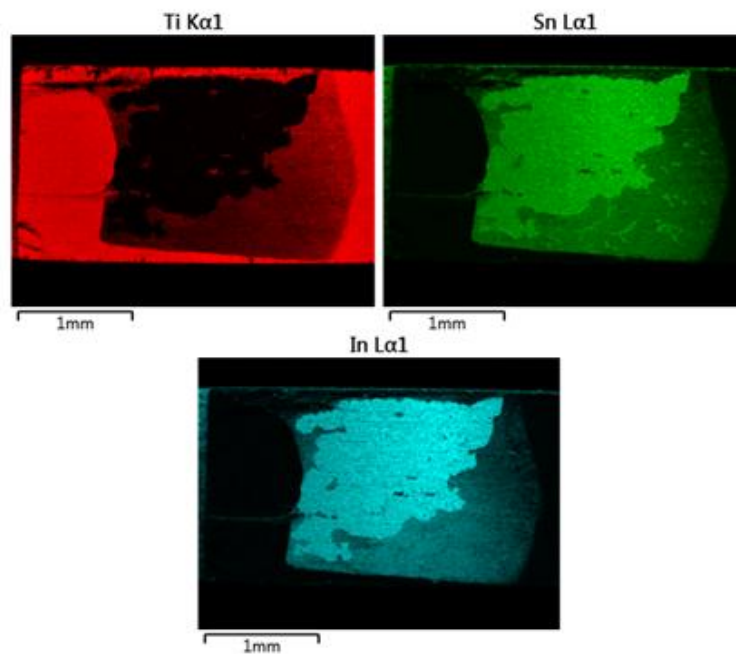
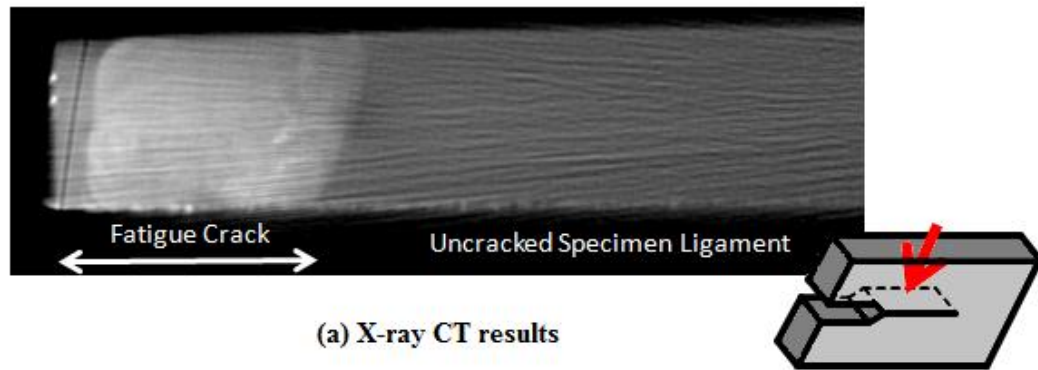


Figure 7. Evidence of healing material in crack mouth. (a) CT scan image of healed crack. (b) EDS image of material on crack faces. Note that (a) and (b) show results from two different specimens.

Summary

A crack healing system for metallic aerospace alloys is proposed where the protected material or component is coated with a low-melting-temperature metallic material. After crack damage occurs, the component is heated to melt the healing film, which then flows into the crack opening. Upon solidification, the healing material serves to mitigate crack damage in two ways. First, while the healing material is intact, tensile forces are transmitted across the crack faces as if the crack faces were glued or welded together. This mechanism, termed “crack

bridging” reduces the crack-tip driving force (ΔK) which in turn reduces the crack growth rates. After the healing material is damaged or ruptured, the presence of residual healing material in the crack mouth causes premature contact of crack faces. This process is an artificial crack closure mechanism.

Experimental results have shown that, during fatigue crack growth of a titanium alloy (Ti 6-2-2-2), crack arrest is possible at crack-tip loads of $\Delta K = 6.6 \text{ MPa}\sqrt{\text{m}}$. Although no permanent crack arrest occurs at higher ΔK (*i.e.*, $13.2 \text{ MPa}\sqrt{\text{m}}$), the data show that a significant reduction (on the order of 50%) in crack growth rate still occurs. Furthermore, the process is repeatable in inert environments in that a single healing film can be reused.

References

- (1) J.A. Newman, P.E. Leser, T.A. Wallace, and S.W. Smith, “The Arrest and Propagation of Fatigue Cracks Using Thin-film Healing Materials,” presented at the 24th Advanced Aerospace Materials and Processes (AeroMat) Conference and Exposition, April 2-5, 2013, Bellevue, Washington.
- (2) FAA, Aviation Maintenance Technician Handbook–Airframe, Vol. 1 Ch. 4 FAA-H-8083-31 (2012) pp. 92-114.
- (3) A.R. Hamilton, N.R. Sottos, and S.R. White, “Self-healing of Internal Damage in Synthetic Vascular Materials,” *Adv. Mater.* 22 (2010) pp. 5159-5163.
- (4) D.A. Hurley and D.R. Huston, “Coordinated Sensing and Active Repair for Self-healing,” *Smart Mater. Struct.* 20 (2011).
- (5) C.J. Norris, J.A.P. White, G. McCombe, P. Chatterjee, I.P. Bond, and R.S. Trask, “Autonomous Stimulus Triggered Self-healing in Smart Structural Composites,” *Smart Mater. Struct.* 21 (2012) pp. 1-10.
- (6) A.J. Patel, N.R. Sottos, E.D. Wetzel, and S.R. White, “Autonomic Healing of Low-velocity Impact Damage in Fiber-reinforced Composites,” *Composites A* 41 (2010) pp. 360-368.
- (7) K.S. Toohy, N.R. Sottos, J.A. Lewis, J.S. Moore, and S.R. White, “Self-healing Materials with Microvascular Networks,” *Nature Mater.* 6 (2007) pp. 581-585.
- (8) Y. Yang and M.W. Urban, “Self-healing Polymeric Materials,” *Chem. Soc. Rev.* 42 (2013) pp. 7446-7467.
- (9) D.Y. Wu, S. Meure, and D. Solomon, “Self-healing Polymeric Materials: A Review of Recent Developments,” *Progress in Polymer Science* 33 (2008) pp. 479-522.
- (10) M.V. Manuel, “Principles of Self-healing in Metals and Alloys: An Introduction,” *Self-healing Materials: Fundamentals, Design Strategies and Applications*, Wiley (2009) pp. 251-265.
- (11) M.V. Manuel, “Biomimetic Self-healing Metals,” *Proceedings for the 1st International Conference on Self-healing Materials*, Series in Materials Science, vol. 100, Spring, Noordwijk aan Zee, 18-20 April 2007.
- (12) M.C. Wright, M.V. Manuel, and T.A. Wallace, “Fatigue Resistance of Liquid-assisted Self-repairing Aluminum Alloys Reinforced with Shape Memory Alloys,” NASA/TM-2013-217925, 2013.
- (13) M. Nosonovsky and P.K. Rohatgi, “Biomimetics in Material Science: Self-healing, Self-lubricating, and Self-cleaning Materials,” *Springer Series in Materials Science* 152 (2012) pp. 44-48.
- (14) S. Hautakangas, et al., “Self-healing Behavior in Man-made Engineering Material: Bioinspired but Taking into Account their Intrinsic Character,” *Phil. Trans. R. Soc. A* 367 (2009) pp. 1689-1704.
- (15) R.N. Lumley and I.J. Polmear, “Advances in Self-healing Metals,” *Proceedings for the 1st International Conference on Self-healing Materials*, Series in Materials Science, vol. 100, Spring, Noordwijk aan Zee, 18-20 April 2007.
- (16) R.N. Lumley, I.J. Polmear, and A.J. Morton, “Interrupted Aging and Secondary Precipitation in

- Aluminum Alloys," *Mater. Sci. Technol.* 19 (2003) pp. 1483-1490.
- (17) S. Hautakangas, H. Schut, N.H. van Dijk, P.E.J. Rivera Diaz del Castillo, and S van der Zwaag, "Self-healing of Deformation Damage in Underaged Al-Cu-Mg Alloys," *Scripta Materialia* 58 (2008) pp. 719-722.
 - (18) S. Hautakangas, H. Schut, S. van der Zwaag, P.E.J. Rivera Diaz del Castillo, and N.H. van Dijk, "Positron Annihilation Spectroscopy as a Tool to Develop Self-healing in Aluminum Alloys," *Phys. Stat. Sol.* 4 (2007) pp. 3469-3472.
 - (19) R.J.H. Wanhill, "Fatigue Crack Initiation in Aerospace Aluminum Alloys, Components and Structures," *Proceedings fo the 1st International Conference on Self-healing Materials, Series in Materials Science*, vol. 100, Spring, Noordwijk aan Zee, 18-20 April 2007.
 - (20) W.G. Moffatt, *The Handbook of Binary Phase Diagrams*, General Electric Co., Schenectady, NY, 1981 (vol. 4)
 - (21) R.S. Piascik, J.C. Newman, Jr., and J.H. Underwood, "The Extended Compact Tension Specimen," *Fatigue and Fracture of Engineering Materials and Structures*, 20 (1997) pp. 559-563.
 - (22) ASTM, *Standard Test Method for Measurement of Fatigue Crack Growth Rates*, Annual Book of ASTM Standards, Vol. 3.01, E647, 2010.
 - (23) W.F. Deans, C.B. Jolly, W.A. Poyton, and W. Watson, "A Strain Gauging Technique for Monitoring Fracture Mechanics Specimens During Environmental Testing," *Strain*, Vol. 13, 1977, pp. 152-154.
 - (24) J.C. Newman, Jr., Y. Yamada, and M.A. James, "Stress-intensity-factor Equations for Compact Specimen Subjected to Concentrated Forces," *Engineering Fracture Mechanics*, 77 (2010) pp. 1025-1029.
 - (25) W.T. Riddell and R.S. Piascik, "Stress Ratio Effects on Crack Opening Loads and Crack Growth Rates in Alumium Alloy 2024," *ASTM STP 1332*, T.L. Panontin and S.D. Sheppard, Eds., American Society for Testing and Materials, West Conshohocken, Pennsylvania, 1999, pp. 407-425.
 - (26) J.A. Newman, "The Effects of Load Ratio on Threshold Fatigue Crack Growth in Aluminum Alloys," Ph.D. dissertation, Virginia Polytechnic Institute and State University, Blacksburg, Virginia, 2000.
 - (27) Y.C. Chen and C.C. Lee, "Indium-copper multilayer Composites for Fluxless Oxidation-free Bonding," *Thin Solid Films*, Vol. 283 (1996) pp. 243-246.
 - (28) B.S. Lee, et al., "Piezoelectric MEMS Generators Fabricated with an Aerosol Deposition PZT Thin Film," *J. Micromech. Microeng.* Vol 19 (2009).
 - (29) X.Y. Wang, et al., "A Micrometer Scale and Low Temperature PZT Thick Film MEMS Process Utilizing an Aerosol Deposition Method," *Sensors and Actuators, A* 143 (2007) pp. 469-474.

APPENDIX – Healing Film Application and Characterization

Details of the healing film sputter deposition process, as well as some film characterization studies are presented in this appendix. For brevity in the main body of the paper, this information is presented as an appendix.

Healing Film Sputter Deposition Process

A radio frequency (RF) sputter deposition technique was utilized for the application of the metallic healing film. A deposition rate of $\sim 1 \mu\text{m/hr}$ for 5-15 hours was used with a power of 250 W, resulting in film thicknesses on the order of $\sim 5\text{-}15 \mu\text{m}$. Upon completion of the film deposition, the specimens were annealed at 135°C for thirty minutes to help consolidate the film. Deposition took place in an inert argon environment with pre-backfill pressures on the order of $1.3 \times 10^{-4} \text{ Pa}$ ($1 \times 10^{-6} \text{ Torr}$) and an argon pressure of approximately 1.1 Pa (8 mTorr). After the chamber was pumped down and backfilled with inert gas, specimens were etched for 10 minutes with a power of 125W to remove surface oxides and promote better film adhesion.

Typically, sputter coating processes are used to deposit films much thinner than the targeted range of 5-15 μm of this study. New deposition methods better suited for thick films have been developed in the Microelectromechanical Systems (MEMS) field. Of notable mention is the aerosol deposition technique, which is currently being investigated for its utility in applying the healing material quickly and in relatively large thicknesses (refs. 28, 29). Since sputter times tended to be long, overheating was a constant concern. Therefore, the sputtering deposition had to be done in layers for two hours or less, with at least one hour of cooling time. Due to these time constraints, approximately one healing coating could be deposited per week, with the possibility of coating up to four specimens per deposition along with witness samples. Typical runs consisted of only two single-edge notch tension (ESE(T)) specimens along with witness samples as shown in Figure A1. The witness samples were small coupons of material with the same healing film as the crack growth specimens. Scanning electron microscope (SEM) analysis and scratch tests were conducted to evaluate the quality of the In-Sn deposited film.

A diagram highlighting the basic coating process can be seen in Figure A2. The “target” is essentially a disk of material that is to be deposited on the substrate, which sits on the stage as shown. A plasma is initiated in the chamber which propels ions at the target, dislodging atomic-scale particles of, in this case, 60/40 In-Sn. The particles then travel back toward the substrate, coating it uniformly over time. The target and the gun assembly are the main concern when dealing with overheating. Due to the low melting temperature of the eutectic alloy (as is required for practical healing of many aerospace components), overheating can cause the target to melt, potentially ruining any specimens in the chamber and, more seriously, causing direct etching of the copper contact on the gun itself once the target is spent. The gun’s copper contact is all that stands between the high vacuum chamber and the water cooling system within the gun; damage to the copper plating and an ensuing water leak could result in mechanical failure of the vacuum system.

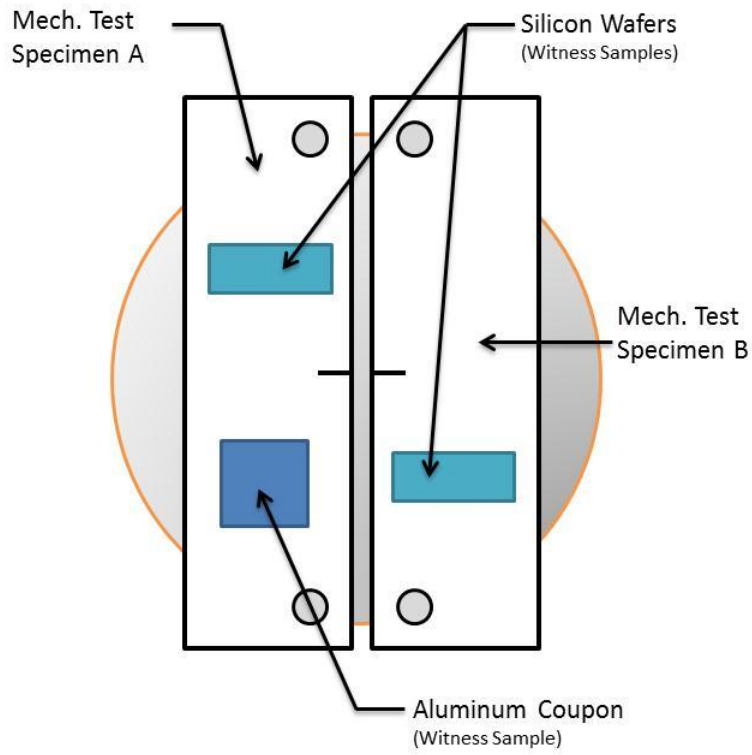


Figure A1. Typical specimen configuration for sputter deposition process.

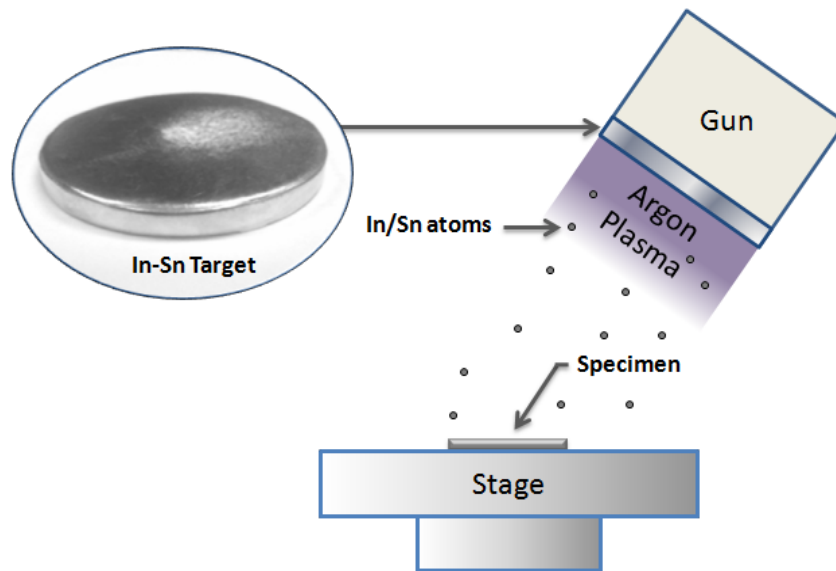


Figure A2. Schematic of sputter deposition system.

Film Analysis and Scratch Testing

As shown in Figure A1, square aluminum specimens were also coated with a thin layer of the In-Sn alloy (approximately 5-15 μm thick). These witness specimens were mechanically polished before being placed in the sputtering chamber, as was done for the fatigue crack growth specimens, in order to ensure that the film quality was consistent. It should be noted that aluminum was originally used in place of titanium in all experiments until a switch to titanium was made for temperature robustness. Due to availability, use of the aluminum witness samples was continued. However, during the study, it became apparent that wetting characteristics were a critical aspect of the healing process, and, therefore, future work will match the substrate material of witness samples to that of the crack growth test specimens. In addition to the aluminum coupons, silicon witness coupons were also coated for purposes of measuring true film thickness. These silicon specimens were notched on the back side so that they could be broken post-deposition, exposing a clean film cross-section which could then be dimensioned and characterized using an SEM. A typical cross-section of a healing film is shown in Figure A3; for this particular cross-section, the film thickness was measured to be between 5.28 and 5.88 μm . Additionally, the quality of the film could be characterized; specifically, the void content within the In-Sn film. A quartz gage was available for thickness measurements inside the sputtering chamber, but the heavy coatings of metal being applied relatively constantly over the course of the experiment made the quartz gage difficult to maintain, so the witness sample was deemed more reliable (recall, the films applied in this study are significantly thicker than typical applications using sputter deposition.)

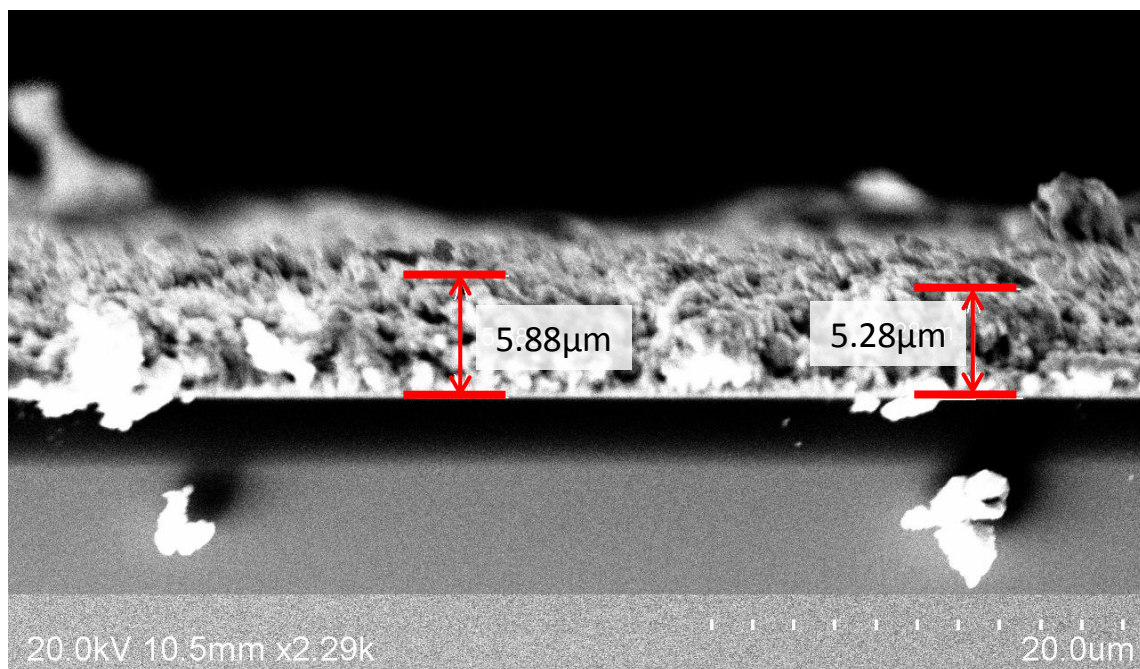


Figure A3. Typical cross-section of a sputter deposited In-Sn film.

To characterize the performance of the healing film, “scratch tests” were performed on the aluminum witness specimens in an SEM equipped with a heating stage. These specimens were scratched with a pair of tweezers before being installed in the microscope to expose some of the substrate beneath the film. This was an attempt to provide a region for flow to be observed, although it should be noted that the scratched region would also oxidize since the scratching was performed in air. Specimens were then heated to the melting point of the healing material, and the resulting molten material was expected to flow into the scratched regions. An example of this can be seen in Figure A4. Here, some of the In-Sn material flowed into the scratch in the form of large beads, while other regions of the In-Sn film did not appear to melt. Presumably, the area that didn’t melt was oxidized material with a significantly higher melting temperature. It is believed that an ideal healing film would allow In-Sn material to flow into a scratch or crack uniformly over its area. More work is needed to study the In-Sn film characteristics that limit the appearance of molten material to a few discrete locations. Eliminating these features should lead to better performance of the healing film.

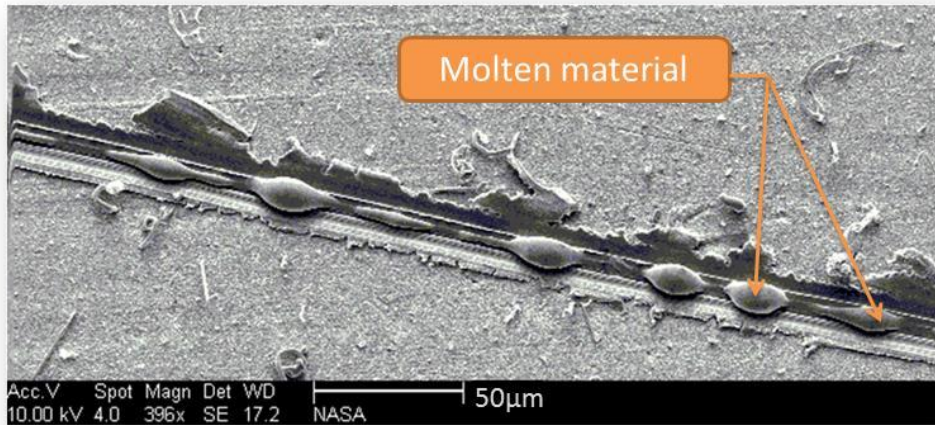


Figure A4. Results of a scratch test on an In-Sn witness specimen (aluminum substrate).

REPORT DOCUMENTATION PAGE				Form Approved OMB No. 0704-0188	
<p>The public reporting burden for this collection of information is estimated to average 1 hour per response, including the time for reviewing instructions, searching existing data sources, gathering and maintaining the data needed, and completing and reviewing the collection of information. Send comments regarding this burden estimate or any other aspect of this collection of information, including suggestions for reducing this burden, to Department of Defense, Washington Headquarters Services, Directorate for Information Operations and Reports (0704-0188), 1215 Jefferson Davis Highway, Suite 1204, Arlington, VA 22202-4302. Respondents should be aware that notwithstanding any other provision of law, no person shall be subject to any penalty for failing to comply with a collection of information if it does not display a currently valid OMB control number.</p> <p>PLEASE DO NOT RETURN YOUR FORM TO THE ABOVE ADDRESS.</p>					
1. REPORT DATE (DD-MM-YYYY) 01-05 - 2014		2. REPORT TYPE Technical Memorandum		3. DATES COVERED (From - To)	
4. TITLE AND SUBTITLE Mitigation of Crack Damage in Metallic Materials			5a. CONTRACT NUMBER		
			5b. GRANT NUMBER		
			5c. PROGRAM ELEMENT NUMBER		
6. AUTHOR(S) Leser, Patrick E.; Newman, John A.; Smith, Stephen W.; Leser, William P.; Wincheski, Russell A.; Wallace, Terryl A.; Glaessgen, Edward H.; Piascik, Robert S.			5d. PROJECT NUMBER		
			5e. TASK NUMBER		
			5f. WORK UNIT NUMBER 432938.11.01.07.43.98.09		
7. PERFORMING ORGANIZATION NAME(S) AND ADDRESS(ES) NASA Langley Research Center Hampton, VA 23681-2199			8. PERFORMING ORGANIZATION REPORT NUMBER L-20418		
9. SPONSORING/MONITORING AGENCY NAME(S) AND ADDRESS(ES) National Aeronautics and Space Administration Washington, DC 20546-0001			10. SPONSOR/MONITOR'S ACRONYM(S) NASA		
			11. SPONSOR/MONITOR'S REPORT NUMBER(S) NASA/TM-2014-218272		
12. DISTRIBUTION/AVAILABILITY STATEMENT Unclassified - Unlimited Subject Category 26 Availability: NASA CASI (443) 757-5802					
13. SUPPLEMENTARY NOTES					
14. ABSTRACT A system designed to mitigate or heal crack damage in metallic materials has been developed where the protected material or component is coated with a low-melting temperature film. After a crack is formed, the material is heated, melting the film which then infiltrates the crack opening through capillary action. Upon solidification, the healing material inhibits further crack damage in two ways. While the crack healing material is intact, it acts like an adhesive that bonds or bridges the crack faces together. After fatigue loading damages, the healing material in the crack mouth inhibits further crack growth by creating artificially-high crack closure levels. Mechanical test data show that this method successfully arrests or retards crack growth in laboratory specimens.					
15. SUBJECT TERMS Adhesives; Bonding; Coatings; Crack; Crack opening displacement; Damage					
16. SECURITY CLASSIFICATION OF:			17. LIMITATION OF ABSTRACT	18. NUMBER OF PAGES	19a. NAME OF RESPONSIBLE PERSON
a. REPORT	b. ABSTRACT	c. THIS PAGE			STI Help Desk (email: help@sti.nasa.gov)
U	U	U	UU	21	19b. TELEPHONE NUMBER (Include area code) (443) 757-5802